RFI Mitigation / Excision Techniques

D. Anish Roshi

NRAO, Green Bank

Abstract

Radio frequency interference (RFI) is increasingly affecting radio astronomy research. A few years ago, active research to investigate the possibility of observing in the presence of interference using RFI mitigation techniques was initiated. In this paper, I briefly discuss four RFI mitigation/excision projects. These projects are: (1) A technique to suppress double sideband amplitude modulated interference using which I show that an astronomical signal in the presence of a DSB interference can be observed with a signal-to-noise ratio a factor of 2 less compared to observations if the RFI were not present. (2) Techniques to suppress interference due to synchronization signals in composite video signals are presented. A combination of noise-free modeling of the synchronization signals and adaptive filtering is used for suppressing the interference. (3) Design techniques to minimize spurious pick-up at the analog input of an Analog-to-digital converter are discussed. (4) Spectral RFI excision using a spectral channel weighting scheme and its application to Green Bank Telescope observations are also presented.

1 Introduction

The need to find ways to deal with radio frequency interference (RFI) is becoming more urgent because: (1) increase in research interests outside the allocated frequency bands for radio astronomy and (2) growing technological resources which are potential sources of radio frequency interference. Spectrum regulations alone cannot help future astronomy research. Active research was started a few years ago to investigate the possibility of doing radio astronomy observations in the presence of interference using RFI mitigation techniques. Several new mitigation techniques have been developed and applied on radio astronomy data in the past few years [1 and references therein].

In this paper I briefly discuss four RFI mitigation/excision projects. These projects are (1) technique to suppress double sideband (DSB) interference; (2) technique to cancel composite video signal interference; (3) design of a "clean" Analog-to-Digital converter (ADC) and (4)spectral RFI excision.

2 'DSB suppressor'

Consider an astronomically interesting spectral feature (for example, a red-shifted HI feature; see Fig. 1) at the upper sideband side of a DSB modulated interference. The output of the radio telescope can be written as

$$y(t) = I_c \cos(\omega_c t)\,[1 + I_m \cos(\omega_m t)] + n(t) \tag{1}$$

where, I_c & ω_c are the amplitude and angular frequency of the carrier signal, I_m & ω_m are the amplitude and angular frequency of the modulating signal and $n(t)$ is the astronomical signal. For simplicity, we consider only one Fourier component of the modulating signal. Multiplying $y(t)$ with $\sin(\omega_c t)$ gives

$$y'(t) = \frac{I_c}{2} \sin(2\omega_c t)\,[1 + I_m \cos(\omega_m t)] + n(t)\sin(\omega_c t) \tag{2}$$

Equation (2) shows that after multiplication the interfering signal will be present only at $2\omega_c$ and not at the baseband. The astronomical signal $n(t)$ is essentially a Gaussian random noise. Multiplying $n(t)$ with $\sin(\omega_c t)$ therefore produces noise signals at $(\omega + \omega_c)$ and $(\omega - \omega_c)$ frequencies. The noise at $(\omega + \omega_c)$ is contaminated by interference. The noise at $(\omega - \omega_c)$ frequency is at the baseband free of any interference (see Fig. 1). However, at the baseband, the noise below ω_c folds back resulting in a degradation of the signal-to-noise ratio by 2 compared to the detection of the astronomical signal in single sideband mode in the absence of the interfering signal.

In reality, the phase of the carrier frequency changes with time due to a variety of reasons, like for instance propagation effects. This change has to be taken into account by the suppressor for effective RFI rejection. This is done by filtering the

[1]The National Radio Astronomy Observatory is a facility of the National Science Foundation operated under cooperative agreement by Associated Universities, Inc.

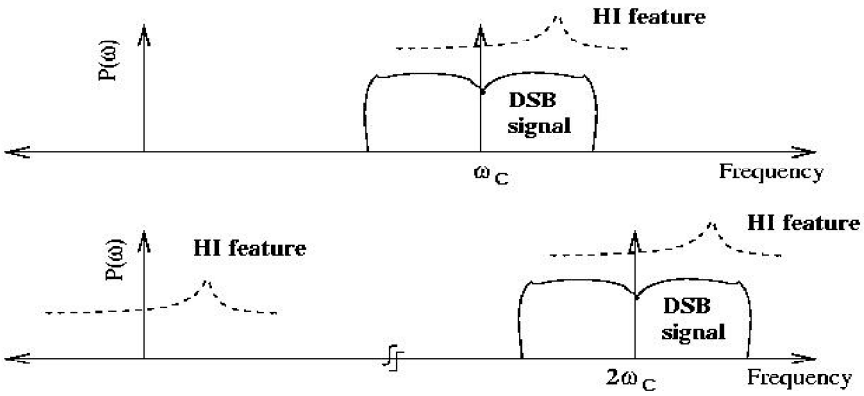

Figure 1: Schematic of the power spectrum of a double sideband (DSB) modulated interference along with an HI feature (top). The carrier frequency of the DSB interference is ω_c. The bottom figure shows a schematic of the spectrum after multiplying the RFI contaminated signal with the quadrature of the carrier of the DSB interference. The DSB interference is translated to $2\omega_c$ due to the multiplication. The astronomical signal will be present at the baseband as well as near $2\omega_c$ after multiplication. Thus low-pass filtering the multiplied output will give the astronomical signal without any RFI contamination. The spectral components of the astronomical signal and any noise below the carrier frequency, however, folds back in frequency at the baseband. This results in the degradation of signal-to-noise ratio by a factor of 2 compared to the case when the astronomical signal is observed in the absence of DSB interference.

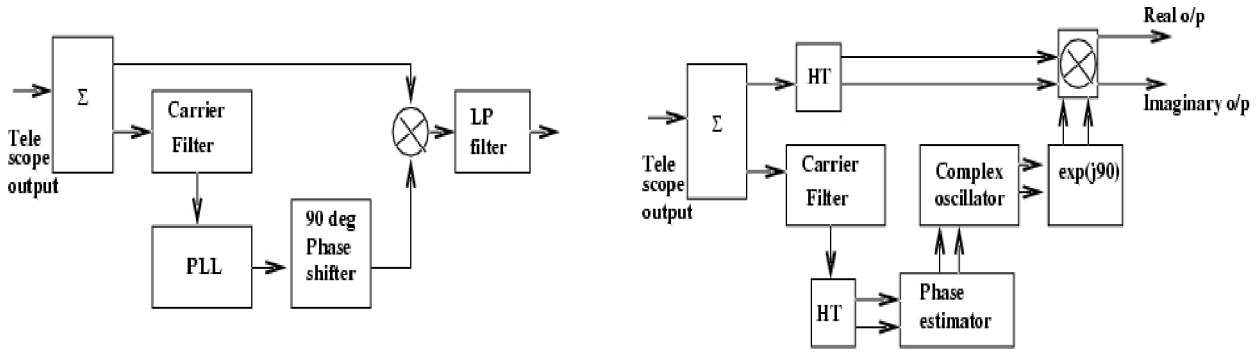

Figure 2: Simplified block diagrams of a 'DSB suppressor' (left) and its MATLAB implementation (right).

carrier signal from the output of the telescope and phase locking with an oscillator (see Fig. 2). The oscillator is then phase shifted by 90^o and mixed with the telescope output. The mixer output is low-pass filtered to get the desired astronomy signal. We implemented a variation of this technique in MATLAB, where a Hilbert transform of the telescope output is taken first to convert it into an analytic signal. This signal is then multiplied with a complex oscillator, which is phase locked to the carrier. The output of the multiplier is now a complex signal. The real part of the complex output ('real' output) is equivalent to that described above. The imaginary part of the complex output ('imaginary' output) is equivalent to the telescope output being multiplied by the oscillator signal with 0^o phase shift with respect to the carrier – essentially a coherent detector.

The performance of the 'DSB suppressor' is measured using a data set consisting of DSB modulated video signal in NTSC format (see Section. 3.1 for details on the data). Fig. 3 shows the result of the performance test. The measured *lower limit* on the interference rejection is $\sim$ 12 dB. The limitations of the 'DSB suppressor' are: (1) good suppression can be achieved only if both sidebands are of equal amplitude and their relative phase is as expected theoretically and (2) any non-DSB noise from the interfering source will degrade the system temperature of the radio telescope. From an observational point of view, the DSB suppressor is good for continuum observations. For spectroscopic observations, the spectral feature should be positioned either on the upper or lower side of the carrier frequency. Otherwise the spectral feature gets folded in frequency.

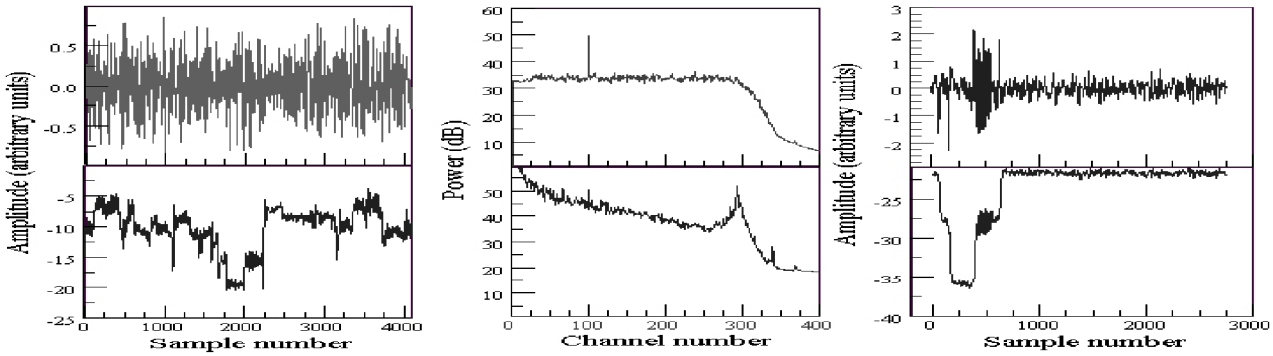

Figure 3: Time series of the 'real' (top-left) and 'imaginary' (bottom-left) outputs when the TV signal is passed through the 'DSB suppressor'. The average spectra (average over 1.6 x 10^5 samples; spectral resolution 12 KHz) of the two outputs are shown in the top-middle and bottom-middle panels respectively. A narrow band signal near channel 100 (top-middle plot), which is a spurious pickup in the ADC and not related with the TV signal, is clearly detected. This pickup is also present in the bottom-middle plot but barely detectable due to interference. The 'real' (top-right) and 'imaginary' (bottom-right) output when a VSB modulated signal is passed through the DSB suppressor is shown on the right. No picture signal is added to the input signal for this plot.

3 Cancellation of Interference due to Composite Video Signal

A considerable fraction of the radio frequency spectrum in the VHF (54 – 88 and 174 – 216 MHz) and the UHF (470 – 890 MHz) bands are allocated for television (TV) transmission. These frequency ranges can be of potential importance for a variety of astronomical observations. For example, the signature of reionization of the Universe is expected as a sharp step in the spectrum of the sky due to red-shifted HI 21-cm line emission anywhere in the frequency range $\sim$ 70 to 240 MHz[2]. Developing techniques to suppress TV signals are thus important. As described below, for TV transmission, a composite video signal is modulated on a carrier. In this section I present techniques to suppress synchronization signals in composite video signal. The suppression of the picture components of composite video signal will be discussed elsewhere.

3.1 Characteristics of TV signal and the data used for the work

TV signals consist of picture and frame synchronization signals and is referred to as composite video signals (see Fig. 4). Synchronization signals consist of horizontal and vertical synchronization and blanking pulses and 8 to 10 cycles of the 3.58 MHz color sub-carrier ('color burst'). The picture part of the composite video signal consists of luminance and chrominance components. The chrominance components are quadrature modulated on a sub-carrier of frequency 3.58 MHz. The total bandwidth of the composite signal is 4.5 MHz. The composite video signal is then vestigial sideband (VSB) modulated on a carrier for transmission. The picture frame rate and other details of the composite video signal depend on the standard used for TV transmission. Here we use data with NTSC standard.

The data for the present work were obtained from the output of a video player. The RF output of the video player was digitized and acquired using a commercial data acquisition system. The carrier frequency of the video player output was near 61.2 MHz and the data were sampled at 50 MHz rate with an 8 bit analog-to-digital converter. A contiguous set of 50 Mbytes of samples was stored in the computer hard disk. Interestingly, the video player output was double sideband (DSB) amplitude modulated. A VSB modulated signal was obtained by appropriately bandpass filtering the recorded data.

3.2 Synchronization signal suppressor

The NTSC TV transmission retains about 1.25 MHz of the lower sideband. Since the spectral power of the synch and blanking pulses increase by more than 10 dB in the frequency range 0 to 1 MHz, the lower sideband in TV transmissions can be used to suppress this power using a 'DSB suppressor'. Thus, after passing the VSB modulated TV signal through the 'DSB suppressor' the 'real' output consists of frequency components all above 1 MHz (see Fig. 3). These components include the color burst and the higher frequency components of the synch and blanking pulses in addition to the picture signal.

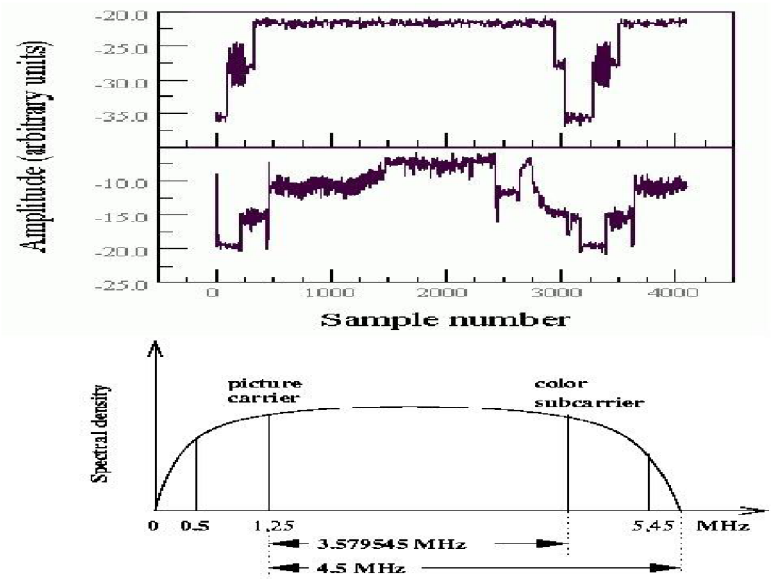

Figure 4: The top panel shows the synchronization signal with no picture information. The largest amplitude pulses are the horizontal synchronization pulses and the intermediate amplitude, wider pulses are the horizontal blanking pulses. The 3.58 MHz color burst is seen just after the synch pulses. The middle panel shows an example of the composite video signal; both picture and synchronization signals are present. A schematic of the spectral details of NTSC TV transmission is shown in the bottom panel. The composite video signal is VSB amplitude modulated on a carrier for transmission.

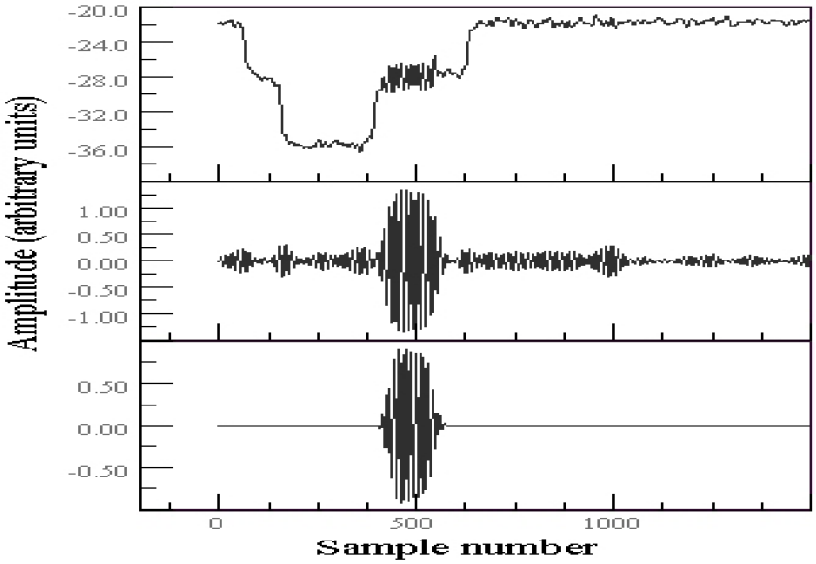

Figure 5: The top panel shows the 'Imaginary' output and the middle panel shows the high pass filtered output of the signal shown in the top panel. The synthesized noise-free model of the color burst is shown in the bottom panel.

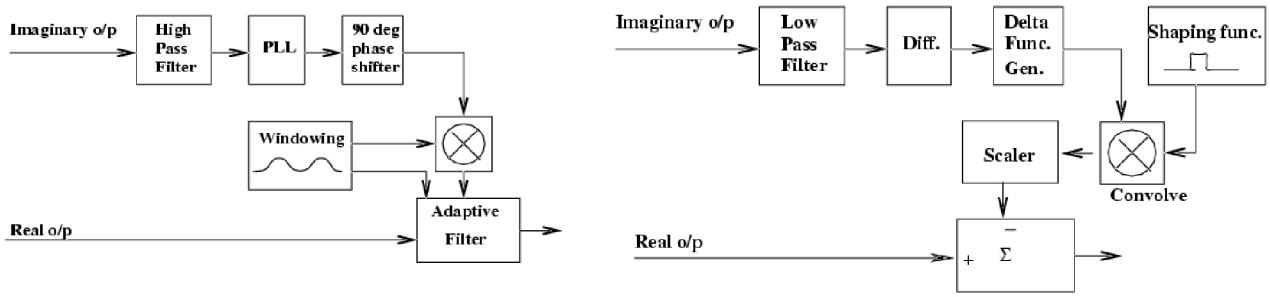

Figure 6: Block diagram of the color burst (left) and synch signal (right) suppressors.

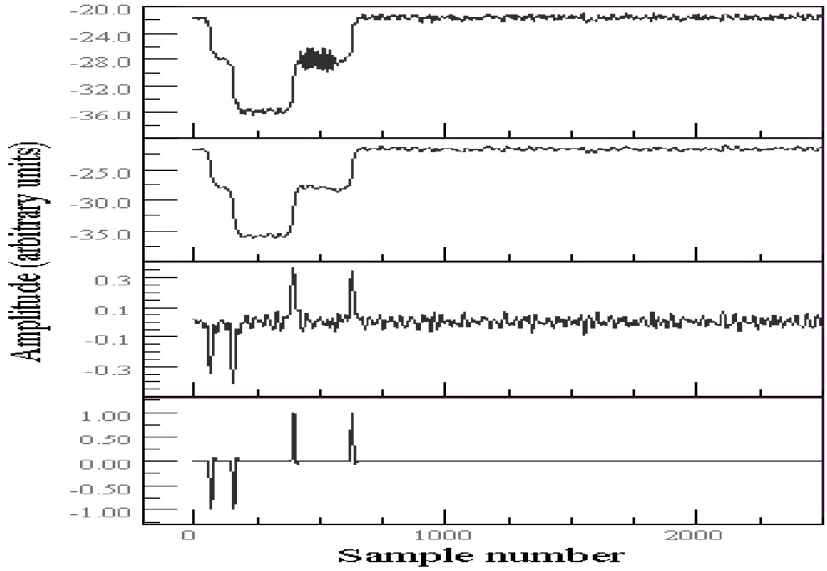

Figure 7: (a)Time series of the 'Imaginary' output. (b) Time series after passing the signal shown in (a) through a low-pass filter. The filter cutoff frequency is adjusted to reject the 3.58 MHz color burst. (c) The derivative of the signal shown in (b). (d) The noise free model of the synch and blanking pulse in the 'Real' output.

We first try to suppress the color burst in the 'real' output by subtracting a noise-free model of this signal. The color burst signal in the 'imaginary' output, which is now considered as a reference signal, is used to make the noise free model. The color burst is filtered out from the 'imaginary' output and used to synchronize the phase of an oscillator (see Figs. 5 & 6). This is done every horizontal synch period where a color burst is present. The oscillator output is then multiplied by a 'window' function to generate the model. The position of the window function in time relative to the horizontal synch signal is estimated in sample numbers and used for synchronizing. The shape of the window function is initially estimated from the reference signal itself and held constant. Subtracting a scaled version of the noise-free model, however, did not give good RFI rejection. Therefore the noise-free model is used as the reference signal for a three tap adaptive filter and the 'real' output is used as the second (main) signal for the filter. New filter weights are computed only during the time interval when the color burst amplitude is not changing rapidly. The need for the adaptive filter is because the shape of the weighting function is changing with time.

After passing the 'real' output through the 'color burst suppressor', what remains are the residuals of synch and blanking pulses. To get a noise-free model for the residual, the synch and blanking pulses from the 'imaginary' output are filtered out first for each horizontal synch period (see Figs. 6 & Fig. 7). Passing the derivatives of these pulses through a threshold detector gives the time of occurrence of these pulses. A 'delta' function model of the residuals is generated using this information. This model is then convolved with a shaping function, which is determined initially from the 'imaginary' output. The noise-free model is then scaled and subtracted from the 'real' output. The scaling factor is adjusted manually to get the best suppression. A typical output after passing the signal through the color burst and synch and blanking pulse

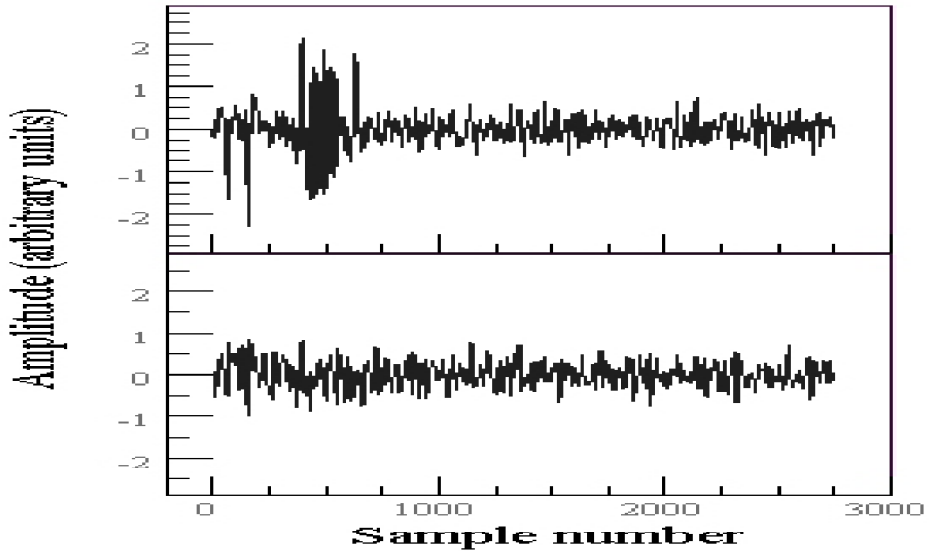

Figure 8: Top panel shows the time series of the 'Real' output. Bottom panel shows the signal after passing the 'Real' output through color burst and synch and blanking pulse suppressors.

suppressors is shown in Fig. 8.

The performance of the synchronization signal suppressors is tested using a data set with no picture information. An average spectrum of the interference is obtained from the samples where the synchronization signals are present in the 'real' output. To measure the achieved RFI rejection, an average spectrum after suppressing the interference is obtained from the same set of samples. These spectra are shown in Fig. 9. The averaging is done over 8.6 x 10^6 samples, which corresponds to about 160 msec. No residual of the color burst is present in the second average spectrum, which gives a lower limit on the interference rejection of 12 dB. The average spectrum of the output of the suppressors is compared with a reference spectrum, which is obtained from the samples with no picture and synchronization signals. The comparison shows good agreement between the reference and average spectrum. The total power in the average spectrum of the output of the suppressors is, however, about 0.6 dB more than that of the reference spectrum. The excess power is mostly due to the inadequate suppression of the synch and blanking pulse residuals.

4 Design of a 'Clean' ADC

The outputs of most commercially available ADCs have spurious components in addition to the digitized form of the desired signal. These spurious components usually appear as narrow band features in the spectrum of the digitized waveform. The spurious components at the output of the ADC limit the performance of the converter for many applications – for example RFI mitigation. The spurious components are due to noise, generated in the associated digital circuits ("digital noise"), coupling to the analog input. The most common reasons for such noise coupling are (a) poor isolation of analog and digital grounds (b) insufficient power supply filtering and (c) poor design of associated digital circuit, which results in excessive ground bounces. In this section I briefly discuss some design techniques to minimize noise coupling to the analog input of an ADC.

4.1 Circuit Design

An analog-to-digital converter circuit is carefully designed to minimize any noise coupling at its analog input using the integrated circuit ADS831 (Burr-Brown product). The ADS831 is an 8 bit ADC. A schematic of the circuit diagram is shown in Fig. 10. The design techniques used to minimize noise coupling are:

1. The ADC is designed to take a balanced analog input. The balanced input is immune to any common mode noise pickup.

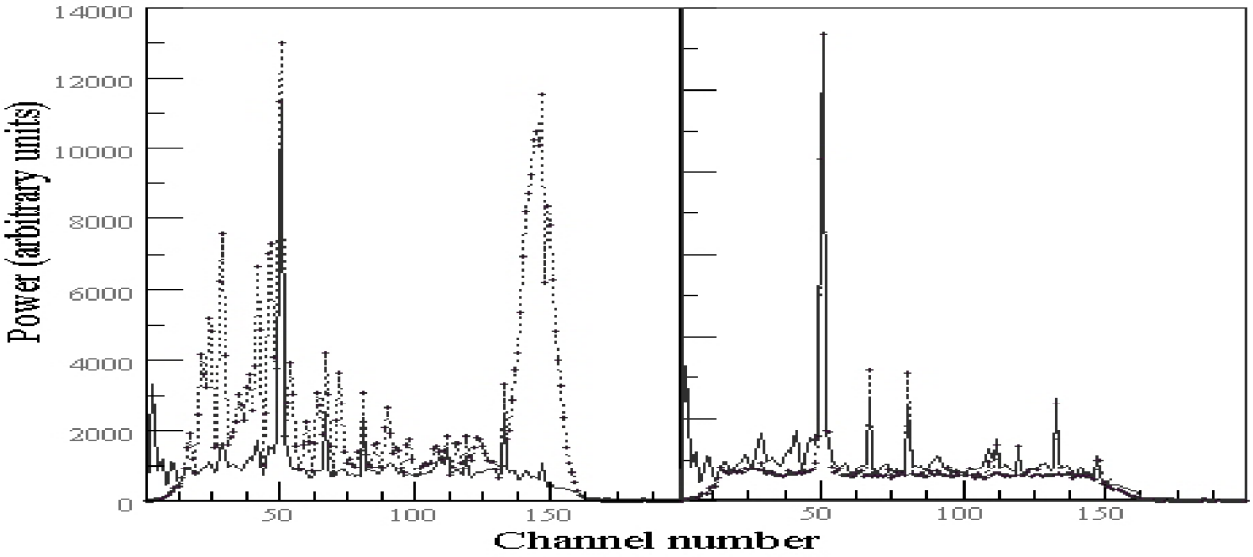

Figure 9: The average spectrum of the samples where interference is present at the 'Real' output is shown on the left panel in dotted line. The average spectrum obtained from the same set of samples after passing the data through the color burst and synch and blanking pulse suppressors is also shown on the left panel in solid line. The spectrum shown in dotted line on the right panel is a reference spectrum, which is obtained from the samples of the 'Real' output that do not have picture or synchronization signals. The average spectrum shown in solid line on the right panel is the same as that shown on the left panel in solid line. The spectra are integrated over 6 x 10^6 samples ($\sim$ 120 msec). The spectral resolution is about 24 KHz.

2. All digital circuitry associated with the ADC is designed to operate at 3.3 V. The low-power supply voltage reduces the digital noise power.

3. Ferrite cores based filters are used for the power supply, which minimizes noise coupling through power connections.

4. Ferrite core based filters are used at the digital power pin of ADS831 for better decoupling.

5. Low-voltage buffers (74LVTH162244) with internal series termination resistors of 25 Ω were used for the design. Also external series resistors are provided (but not used during the tests) at all digital interconnections for better matching of the gate output impedance to the transmission lines (PCB layout). The impedance matching reduces the reflections in the transmission lines thus minimizing ground bounces.

6. The PCB (printed circuit board) is designed such that the analog and digital power/ground planes are separated. The ground planes are interconnected near ADS831 to provide the signal return paths.

7. In the PCB design, the separation between the power planes is 10 and 20 times the separation between the ground and power planes ("20-H rule"[3]).

8. Along with the ADC card, a data acquisition system (DAS) was designed to acquire data from the ADC. Care is taken to isolate DAS ground from the ADC ground and also from the PC ground. The ADC ground and DAS ground are "isolated" using differential line drives (MC100LVELT22) and receivers (MC100LVELT23). The PC ground is optically isolated from the DAS ground. These ground isolations are provided to minimize the digital noise coupling to the ADC circuit.

4.2 Test Results

To test the performance of the ADC, a noise source is connected to its input and the digitized data is acquired using the DAS. The bandwidth of the noise is limited to about 12 MHz and the power level is adjusted such that the ADC output range of 0 to 255 represents roughly 5 times the RMS fluctuations. The data is sampled at 30 MHz. Fig. 11 shows a

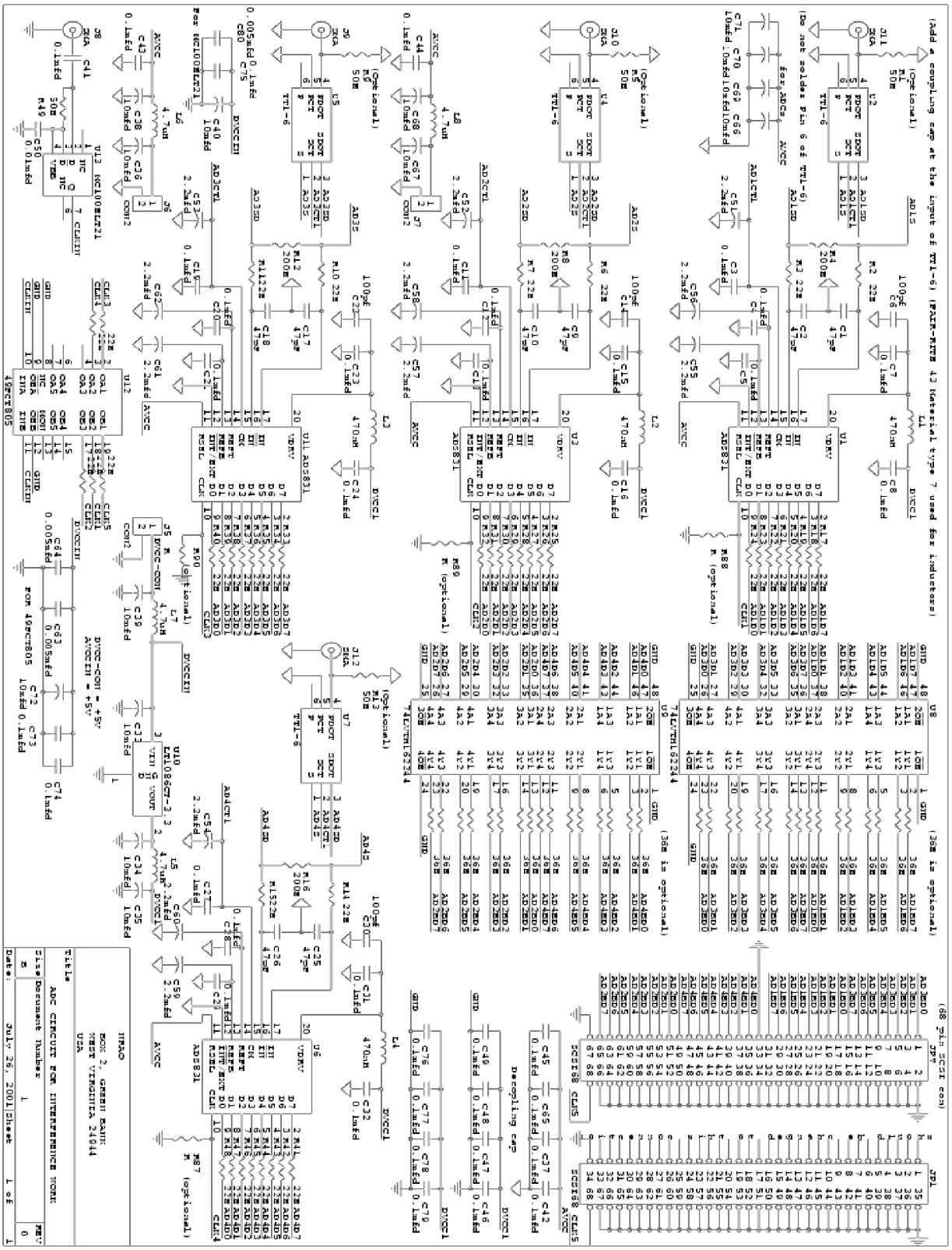

Figure 10: Schematic of the Analog-to-digital converter circuit. The circuit is designed with four ADS831 so that 4 analog inputs can be simultaneously digitized.

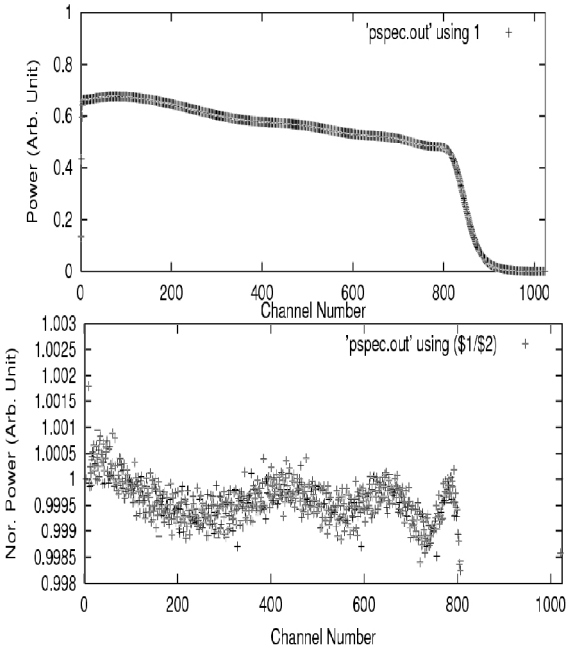

Figure 11: 34 minutes integrated spectrum of the ADC output. To obtain this spectrum, a noise source is connected at the input of the ADC. The integrated bandshape of the noise source is shown on the top and the spectrum after correcting the bandshape is shown on the bottom. No spurious narrow band signals are present at the 3 sigma value of the channel to channel power fluctuations, which corresponds to a spurious level of < -32 dB relative to the noise power.

34 minutes averaged spectrum of the ADC output. To correct the bandshape, the integrated output spectrum is divided by a smoothed (9 point boxcar) version of the same spectrum, which is also shown in Fig. 11. The bandshape corrected spectrum shows that no narrow band spurious signal is present at the output data. The 3 sigma value of the channel to channel power fluctuation in the spectrum corresponds to a spurious suppression better than -32 dB relative to the input noise power. The channel to channel power fluctuation in the averaged spectrum is close to that expected theoretically.

5 Spectral RFI Excision

Spectroscopic observations at low-frequencies ($<$ 1 GHz) are often limited by RFI. Fig. 12 shows an example spectrum over the frequency range 380-420 MHz obtained using the low-frequency receiver of the Green Bank Telescope (GBT). The narrow band features seen in this spectra are RFI. At sufficiently high spectral resolution ($\sim$ 1 KHz), the RFI are usually confined to a few spectral channels and the spectral region between narrow band RFI is often free of any contamination. In addition, some of the RFI are time variable, thus there are time ranges where parts of the spectrum are free of RFI. For certain types of observations only a fraction of the total frequency range of the receiver is needed. An example is the observations of galactic recombination lines (RLs) at low-frequencies. The bandwidth needed for such observations is $\sim$ 1 MHz centered at the expected line frequency (see Fig. 12). This means that RL transitions located at frequencies relatively free of RFI can be observed. Fig. 13 shows four spectra centered at the hydrogen RL transitions H243α (455.4863 MHz), H246α (439.0575 MHz), H249α (423.4093 MHz) and H250α (418.3587 MHz). The spectral resolution and integration time of these spectra are 4.9 KHz and 60 sec respectively. The narrow band features in these spectra are again RFI. In this section, I present a technique to excise the narrow band, time variable RFI using a spectral channel weighting scheme.

5.1 Spectral Channel weighting scheme

To excise RFI a channel weighting scheme is used. In this scheme, at the basic integration level (say 60 sec or less), a weight of unity is assigned to all spectral channels which are "free" of RFI. Fig. 14a&b show respectively an example spectrum and the weights assigned to each channel. The contaminated spectral channels are identified through inspection

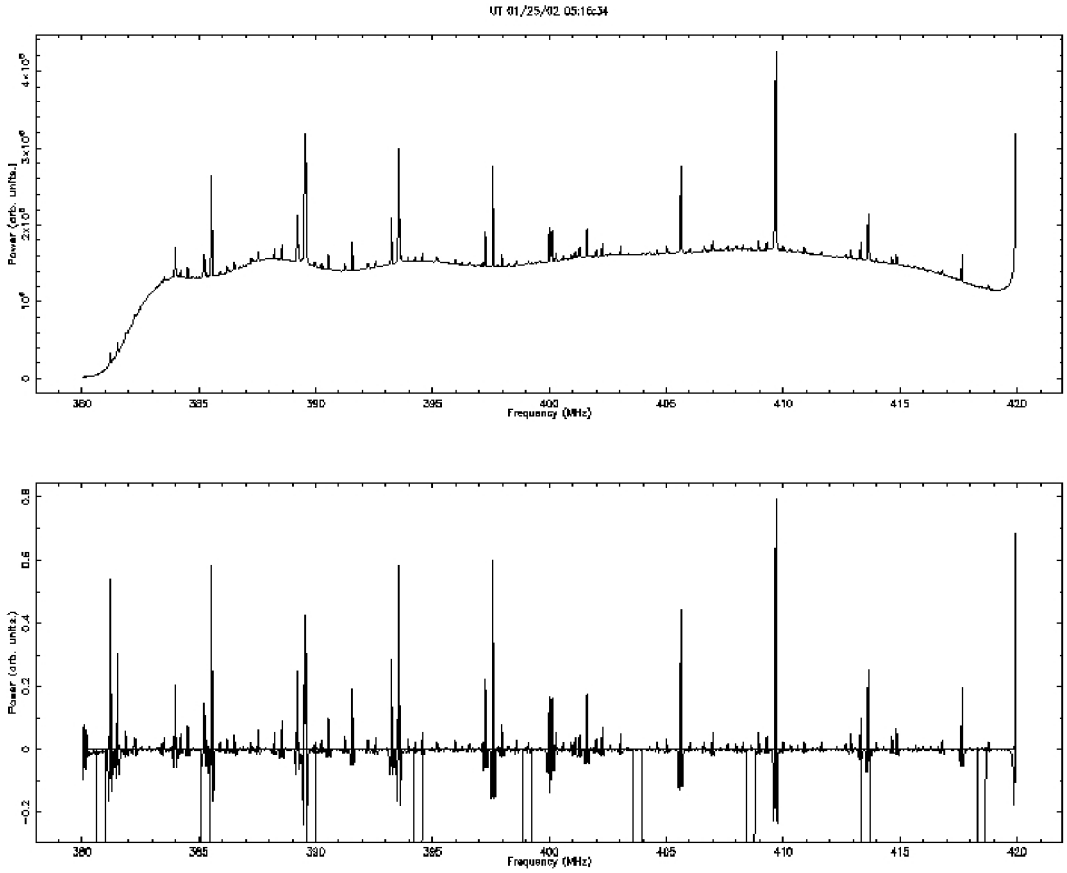

Figure 12: Power spectrum over the frequency range 380-420 MHz obtained from the output of the low-frequency receiver of the GBT (top). The band-shape corrected spectrum is shown on the bottom. The band-shape is obtained by 5 point median filtering the power spectrum shown on top. The spectrum is integrated for about 120 sec. The vertical lines in the bottom spectrum show a 300 KHz spectral window near hydrogen recombination lines.

by eye and their weights are assigned zero. The excision will be made automatic by determining the spectral RMS of the RFI free spectral channel through an iterative process and assigning zero weights to those channels whose spectral amplitudes exceeds a threshold (say 5σ). The final integrated spectrum is obtained by weighted averaging the edited spectra.

5.2 Result of the observations toward G28.4+0.1

With the intention to test the RFI excision scheme, we observed recombination lines toward G28.4+0.1 near 420 MHz with the GBT. Fig 14 shows the RFI excised spectrum obtained toward this source and the corresponding channel weights. For comparison, a spectrum with out any RFI excision is also shown. The effectiveness of the RFI excision scheme is clear from Fig 14.

In the excision scheme, the weights essentially represent the number of points averaged on each channel. Thus non-uniform weights imply that the RMS of the spectral values differ from channel to channel. This has to be taken into account for the estimation of the parameters of the astronomical spectral feature. This will be discussed in detail elsewhere.

Acknowledgment

I thank Rick Fisher and Rich Bradley for the many fruitful discussions I had with them while I worked on this project.

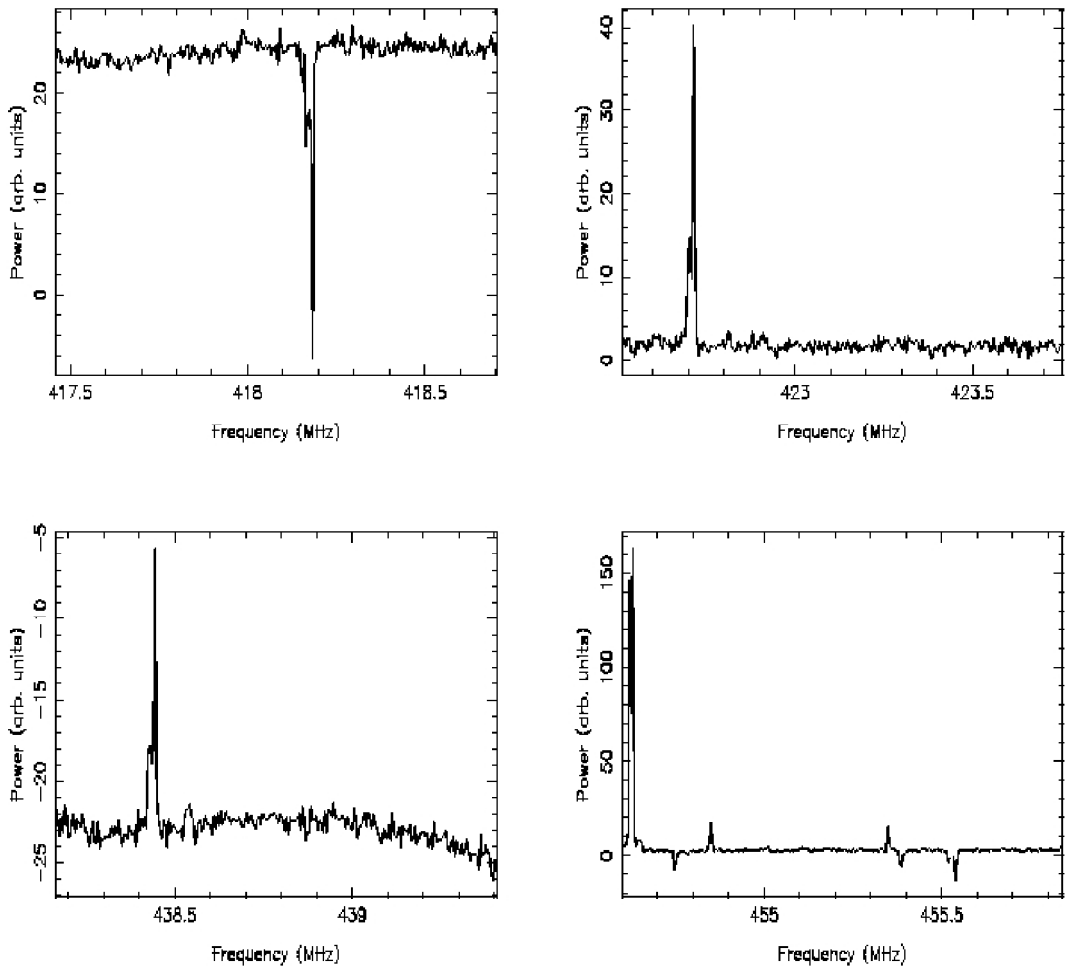

Figure 13: Four 1.25 MHz wide bandshape corrected spectra selected for recombination line observations with the 420 MHz band of the GBT. These bands are centered at hydrogen recombination lines H243α (455.4863 MHz), H246α (439.0575 MHz), H249α (423.4093 MHz) and H250α (418.3587 MHz). The integration time of these spectra are 60 sec. The bandshape is corrected using a reference spectrum, which is obtained by frequency switching.

Reference

[1] Fisher, R. J., 2002, NAIC-NRAO School on Single-Dish Radio Astronomy: Techniques and Applications, ASP conf. series, eds. S. Stanimirovic, D. R. Altschuler, P. F. Goldsmith, C. Salter

[2] P. A. Shaver, R. A. Windhorst, P. Madau, A. G. de Bruyn, 1999, A&A, 345, 380.

[3] Montrose, M. I., 1996, "Printed Circuit Board Design Techniques for EMC Compliance", IEEE Press Series on Electronics Technology, IEEE, Inc., New York.

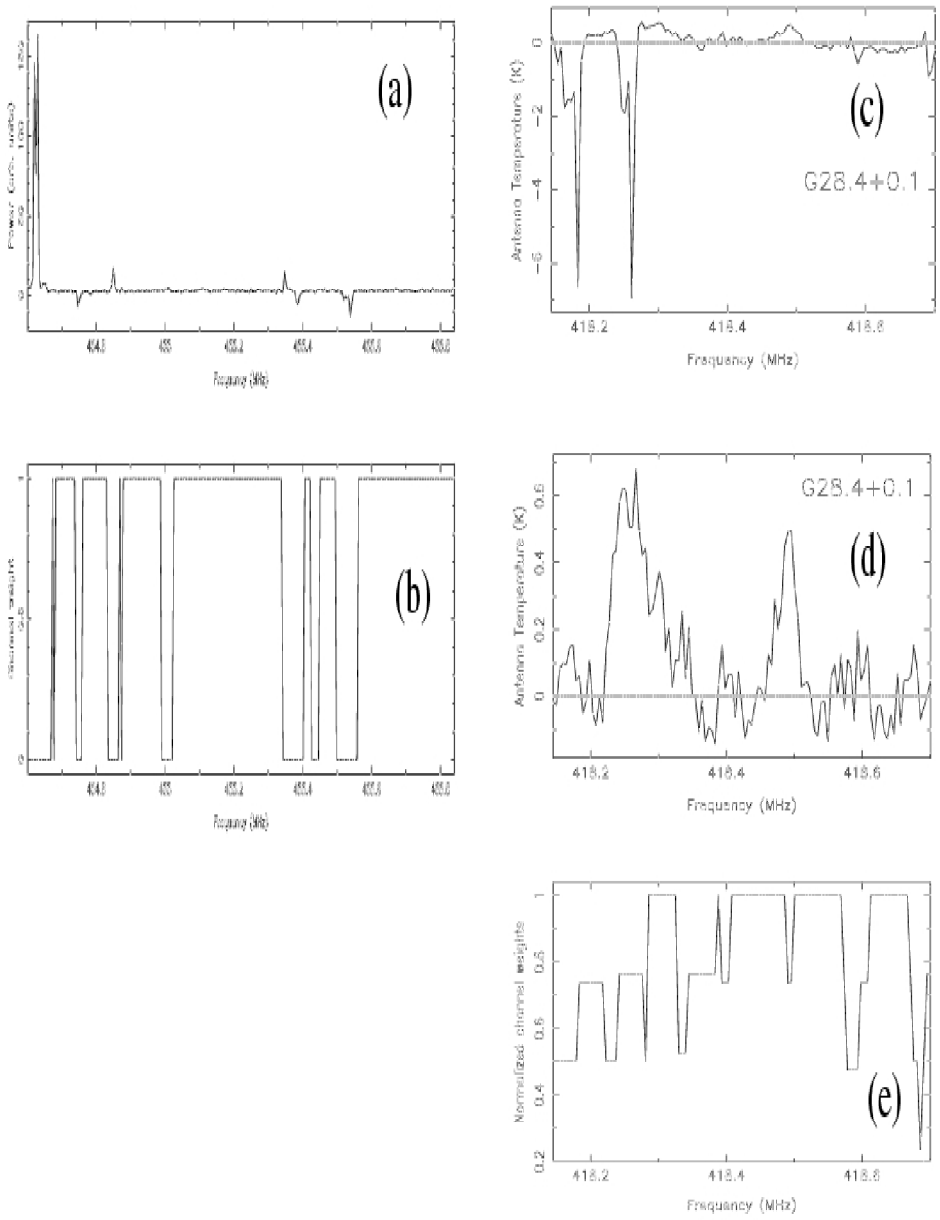

Figure 14: (a)60 sec integrated bandshape corrected spectrum toward G28.4+0.1. The bandshape is corrected using a reference spectrum, which is obtained by frequency switching. (b) The channel weights assigned to each channel at the first stage of editing is plotted as a function of frequency. (c) Average spectrum without any RFI excision. The averaging is done over all integration time and the two transitions H249α (423.4093 MHz) and H250α (418.3587 MHz). The reference spectrum is measured in dual-Dicke frequency switching mode and the plot shows the bandshape corrected 'folded' spectrum. Note that the frequency axis corresponds to the observing band centered at 418.3587 MHz. The bandwidth of the spectrum is only half that of the spectrum shown in (a) because of spectral 'folding'. (d) Average spectrum with RFI excision. The feature near 418.3 MHz is the hydrogen line and that near 418.5 MHz is the carbon line. (e) The normalized channel weights corresponding to the spectrum in (d).